

# *EVII*, a target gene for amplification at 3q26, antagonizes transforming growth factor- $\beta$ -mediated growth inhibition in hepatocellular carcinoma

Kohichiroh Yasui,<sup>1,5</sup> Chika Konishi,<sup>1,5</sup> Yasuyuki Gen,<sup>1</sup> Mio Endo,<sup>1</sup> Osamu Dohi,<sup>1</sup> Akira Tomie,<sup>1</sup> Tomoko Kitaichi,<sup>1</sup> Nobuhisa Yamada,<sup>1</sup> Naoto Iwai,<sup>1</sup> Taichiro Nishikawa,<sup>1</sup> Kanji Yamaguchi,<sup>1</sup> Michihisa Moriguchi,<sup>1</sup> Yoshio Sumida,<sup>1</sup> Hironori Mitsuyoshi,<sup>1</sup> Shinji Tanaka,<sup>2,3</sup> Shigeki Arii<sup>2,4</sup> and Yoshito Itoh<sup>1</sup>

<sup>1</sup>Department of Molecular Gastroenterology and Hepatology, Kyoto Prefectural University of Medicine, Kyoto; <sup>2</sup>Hepato-Biliary Pancreatic Surgery; <sup>3</sup>Molecular Oncology, Tokyo Medical and Dental University, Tokyo; <sup>4</sup>Hamamatsu Rosai Hospital, Japan Labour Health and Welfare Organization, Hamamatsu, Japan

## Key words

Cyclin-dependent kinase inhibitor p15, *EVII*, gene amplification, hepatocellular carcinoma, transforming growth factor  $\beta$

## Correspondence

Kohichiroh Yasui, Department of Molecular Gastroenterology and Hepatology, Kyoto Prefectural University of Medicine, 465 Kajji-cho, Kamigyo-ku, Kyoto 602-8566, Japan.

Tel: +81-75-251-5519; Fax: +81-75-251-0710;

E-mail: yasui@koto.kpu-m.ac.jp

<sup>5</sup>These authors contributed equally to this work.

## Funding Information

Japan Society for the Program of Science.

Received October 31, 2014; Revised April 27, 2015;

Accepted May 2, 2015

*Cancer Sci* 106 (2015) 929–937

doi: 10.1111/cas.12694

*EVII* (ecotropic viral integration site 1) is one of the most aggressive oncogenes associated with myeloid leukemia. We investigated DNA copy number aberrations in human hepatocellular carcinoma (HCC) cell lines using a high-density oligonucleotide microarray. We found that a novel amplification at the chromosomal region 3q26 occurs in the HCC cell line JHH-1, and that *MECOM* (*MDS1* and *EVII* complex locus), which lies within the 3q26 region, was amplified. Quantitative PCR analysis of the three transcripts transcribed from *MECOM* indicated that only *EVII*, but not the fusion transcript *MDS1–EVII* or *MDS1*, was overexpressed in JHH-1 cells and was significantly upregulated in 22 (61%) of 36 primary HCC tumors when compared with their non-tumorous counterparts. A copy number gain of *EVII* was observed in 24 (36%) of 66 primary HCC tumors. High *EVII* expression was significantly associated with larger tumor size and higher level of des- $\gamma$ -carboxy prothrombin, a tumor marker for HCC. Knockdown of *EVII* resulted in increased induction of the cyclin-dependent kinase inhibitor p15<sup>INK4B</sup> by transforming growth factor (TGF)- $\beta$  and decreased expression of c-Myc, cyclin D1, and phosphorylated Rb in TGF- $\beta$ -treated cells. Consequently, knockdown of *EVII* led to reduced DNA synthesis and cell viability. Collectively, our results suggest that *EVII* is a probable target gene that acts as a driving force for the amplification at 3q26 in HCC and that the oncoprotein *EVII* antagonizes TGF- $\beta$ -mediated growth inhibition of HCC cells.

Hepatocellular carcinoma is the third leading cause of cancer death worldwide.<sup>(1)</sup> Several risk factors for HCC have been reported, including infection with hepatitis B and hepatitis C viruses, and alcohol consumption. However, the molecular pathogenesis of this widespread type of cancer remains poorly understood.

Amplification of DNA in certain regions of chromosomes plays a crucial role in the development and progression of human malignancies, specifically when proto-oncogenic target genes within those amplicons are overexpressed. A common criterion for designation of a gene as a putative target of amplification is that gene amplification leads to its overexpression.<sup>(2)</sup>

To identify genes potentially involved in HCC, we investigated DNA copy number aberrations in human HCC cell lines using high-resolution SNP arrays. Here we show that a novel amplification at the chromosomal region 3q26 occurs in an HCC cell line and that the oncogene *EVII*, which lies within the 3q26 region, was amplified.

The *EVII* gene codes for a zinc finger transcriptional factor that plays an important role in normal development and in oncogenesis.<sup>(3)</sup> *EVII* was first identified in mice as the integra-

tion site of an ecotropic retrovirus that leads to murine myeloid leukemia.<sup>(4)</sup> In humans, rearrangements of chromosome 3q26 often activate *EVII* expression in AML, chronic myeloid leukemia, and myelodysplastic syndrome. High *EVII* expression also occurs in AML patients without 3q26 rearrangements, suggesting that other mechanisms of aberrant *EVII* expression exist.<sup>(3)</sup> Importantly, high *EVII* expression is an independent negative prognostic indicator of survival in AML.<sup>(5)</sup> Although the majority of investigations have focused on the contribution of *EVII* to the pathogenesis and clinical characteristics of hematopoietic malignancies, overexpression of *EVII* has also been found in several solid tumors.<sup>(6–8)</sup> However, little is known about its relevance for HCC.

The oncoprotein *EVII* has been reported to influence a number of signaling pathways. Thus, *EVII* activates the PI3K/AKT and RAS/ERK signaling pathways.<sup>(9–11)</sup> Moreover, *EVII* has been reported to suppress TGF- $\beta$  signaling by inhibiting Smad3.<sup>(12)</sup> Transforming growth factor- $\beta$  acts as a tumor suppressor by arresting the growth of cells in the early stages of cancer and, paradoxically, contributes to the phenotype of tumor invasiveness by promoting EMT in the late stages of cancer.<sup>(13)</sup> Transforming growth factor- $\beta$  inhibition of proliferation

is complex and affects a number of signaling targets including CDK inhibitor p15<sup>INK4B</sup> and c-Myc. Briefly, TGF- $\beta$  induces p15<sup>INK4B</sup> expression. The induced p15<sup>INK4B</sup> forms a complex with CDK4 and prevents the activation of CDK4 by cyclin D1, thereby resulting in inhibition of CDK4-mediated Rb phosphorylation. The Rb protein inhibits entry into the cell-division cycle when it is unphosphorylated and, conversely, phosphorylation of Rb by the complex of CDK4 and cyclin D1 encourages cell proliferation. The TGF- $\beta$ -induced p15<sup>INK4B</sup> expression shuts down cell-cycle progression in the early/mid G<sub>1</sub> phase of the cell cycle. Although c-Myc can repress the expression of p15<sup>INK4B</sup>, this action of c-Myc is preemptively blocked by TGF- $\beta$ , which dispatches Smad3 to form a complex with E2F4 or E2F5 plus p107 that represses expression of the c-Myc gene,<sup>(13)</sup> thereby ensuring that TGF- $\beta$  succeeds in inducing the expression of p15<sup>INK4B</sup>. Thus, TGF- $\beta$  influences a number of key signaling molecules to inhibit cell proliferation and suppress the early stages of cancer growth.

Here, we provide evidence that *EV11* is a novel target gene that acts as a driving force for the amplification at 3q26 in HCC and that *EV11* antagonizes the growth inhibition mediated by TGF- $\beta$  in HCC cells.

## Materials and Methods

**Reagents and antibodies.** Antibodies against *EV11* (#2593; C50E12), cyclin D1 (#2922), c-Myc (#5605; D84C12), phospho-Rb (#9308), poly (ADP-ribose) polymerase (#9542), BrdU (#5292; Bu20a), and  $\beta$ -actin (#4967) were purchased from Cell Signaling Technology (Beverly, MA, USA). The antibody against p15<sup>INK4B</sup> (ab53034) was purchased from Abcam (Cambridge, UK). Small interfering RNA duplex oligoribonucleotides targeting *EV11* and negative control siRNA duplexes were purchased from Ambion (Foster City, CA, USA). Human TGF- $\beta$ 1 was obtained from R&D Systems (Minneapolis, MN, USA).

**Cell lines and tumor samples.** Twenty HCC cell lines<sup>(14)</sup> were obtained from ATCC (Manassas, VA, USA) and the JCRB Cell Bank (Osaka, Japan). All cell lines were maintained in DMEM supplemented with 10% FCS. Primary HCC tissues were obtained from patients who underwent surgery at the Hospital of Tokyo Medical and Dental University (Tokyo, Japan). All specimens were immediately frozen in liquid nitrogen and stored at  $-80^{\circ}\text{C}$  until required. Genomic DNA and total RNA were isolated as described previously.<sup>(14)</sup> Sixty-six tumor samples were available for DNA analyses, and 36 paired tumor and non-tumor samples were available for mRNA analyses. The protocol of this study was approved by ethics committees and carried out in accordance with the Declaration of Helsinki. Informed consent was obtained from each patient.

**Array analysis.** DNA copy number changes were analyzed using the GeneChip Mapping 100K array set or the 250K Sty array (Affymetrix, Santa Clara, CA, USA) according to the instructions from the manufacturer, as described previously.<sup>(14,15)</sup>

**Fluorescence *in situ* hybridization.** Fluorescence *in situ* hybridization was carried out using the BACs RP11-721P22 and RP11-137H17 as probes (Invitrogen, Carlsbad, CA, USA), as described previously.<sup>(14)</sup> The BACs were selected based on their homology to locations in the human genome according to the database provided by the University of California Santa Cruz (<http://genome.ucsc.edu/>).

**Real-time Quantitative PCR.** Genomic DNA of *EV11* was quantified using a real-time fluorescence detection method, as

described previously.<sup>(14)</sup> Transcripts of *EV11*, *MDS1-EV11*, and *MDS1* were quantified using the StepOnePlus real-time PCR system (Applied Biosystems, Foster City, CA, USA) and TaqMan universal PCR master mix (Applied Biosystems) with specific primers and TaqMan probes, as described previously.<sup>(7)</sup> The *EV11* probe (against *EV11* exon 1) is designed to specifically recognize *EV11* but not the fusion transcript, *MDS1-EV11*. The *MDS1-EV11* probe recognizes the mRNA fusion site and is specific to *MDS1/EV11*. The *MDS1* probe (against *MDS1* exon 4) recognizes a domain that is not included in the *MDS1-EV11* fusion gene. *ACTB* expression was used as an endogenous control for mRNA levels, and the long interspersed nuclear element 1 was used as an endogenous control for genomic DNA levels. Real-time quantitative RT-PCR experiments for *SERPINE1* (PAI-1), *CDKN2B* (p15<sup>INK4B</sup>), *CCND1* (cyclin D1), *MYC* (c-Myc), and *ITGA1* (integrin  $\alpha$ 1) were carried out, as described previously.<sup>(14)</sup> The sequences of the primers and probes used are shown in Table S1.

**Immunoblotting.** Immunoblotting was carried out as described previously.<sup>(14)</sup> All antibodies were used at dilutions of 1:1000, with the exception of anti- $\beta$ -actin antibody (1:5000). For immunodetection, secondary anti-rabbit IgG or anti-mouse IgG (Amersham, Piscataway, NJ, USA) antibodies were used at a dilution of 1:5000. Antibody binding was detected using the ECL system (Amersham).

**RNA interference and TGF- $\beta$  treatment.** The two siRNAs targeting *EV11* (#1 and #2) and control (non-silencing) siRNA were delivered into cells using Lipofectamine RNAiMAX (Invitrogen), according to the manufacturer's protocol. The medium was replaced with medium without FCS 48 h after transfection, and cells were cultured overnight. A final concentration of 10 ng/mL TGF- $\beta$ 1 or vehicle was then added to medium without FCS. After 24 h of incubation in the presence of TGF- $\beta$ 1, cells were harvested for RT-PCR and immunoblotting analyses, or cells were labeled with BrdU for 6 h. Incorporation of BrdU was determined using the Cell Proliferation ELISA, BrdU (colorimetric) (Roche, Basel, Switzerland). Cell viability was determined using the WST-8 assay (Cell Counting Kit-8; Dojindo, Kumamoto, Japan).

**Enforced expression of *EV11*.** The full-length human *EV11* expression vector (#RC226310) was obtained from OriGene (Rockville, MD, USA). The *EV11* expression vector, or the empty vector, was transfected into cells using the Effectene Transfection Reagent kit (Qiagen, Venlo, Netherlands) according to the manufacturer's instructions. The medium was replaced with medium without FCS 48 h after transfection, and the cells were cultured overnight. Transforming growth factor- $\beta$ 1 at a final concentration of 10 ng/mL was then added to medium without FCS. After 12 h incubation in the presence of TGF- $\beta$ 1, the cells were labeled with BrdU for 12 h and were then analyzed using immunofluorescence.

**Immunofluorescence.** Cells were fixed with 4% paraformaldehyde and were then incubated with a combination of anti-*EV11* (1:500) and anti-BrdU (1:200) antibodies. Alexa Fluor 555-conjugated anti-rabbit IgG and Alexa Fluor 488-conjugated anti-mouse IgG (Cell Signaling Technology) were used to detect the primary antibodies. Nuclei were counterstained with DAPI (Sigma-Aldrich, St Louis, MO, USA). Positive cells were counted.

**Statistical analysis.** Statistical analyses were carried out using SPSS 15.0 software (SPSS, Chicago, IL, USA). Comparisons were made using the Wilcoxon signed-rank test, Student's

*t*-test, ANOVA,  $\chi^2$ -test, or the Mann–Whitney *U*-test. *P*-values < 0.05 were considered to indicate statistical significance.

## Results

**Detection of 3q26 amplicon.** Twenty HCC cell lines were screened for DNA copy number aberrations using GeneChip Mapping 100K and 250K arrays. Gains at the chromosomal region 3q26 were frequently found in 11 (55%) of the 20 cell lines (Fig. 1a). Of these cell lines, JHH-1 cells showed a high-level copy number gain that is indicative of gene amplification at 3q26 (Fig. 1b). The estimated extent of the amplification in JHH-1 cells was approximately 1.0 Mb. This chromosomal region lies between the Affymetrix markers, SNP\_A-1696905 and SNP\_A-1677515, and includes only *MECOM*, which is an officially assigned, but rarely used, gene name (Fig. 1b). *MECOM* consists of *MDS1* and *EV11* genes.

Whereas *EV11* possesses its own transcription start site(s), mRNA transcripts initiating at *MDS1*, located upstream of *EV11*, can splice from exon 2 of *MDS1* into exon 2 of *EV11* to form the fusion transcript, *MDS1–EV11*. Both *MDS1* and *MDS1–EV11* are expressed independently of *EV11*.

To confirm amplification of *MDS1* and *EV11* in JHH-1 cells, these cells were analyzed using FISH with the BACs, RP11-721P22 (containing *EV11*) and RP11-137H17 (containing *MDS1*), as probes. This analysis indicated an increase in the number of RP11-721P22 and RP11-137H17 FISH signals (six signals each) (Fig. 1c). These data confirm that *MDS1* and *EV11* are amplified in JHH-1 cells.

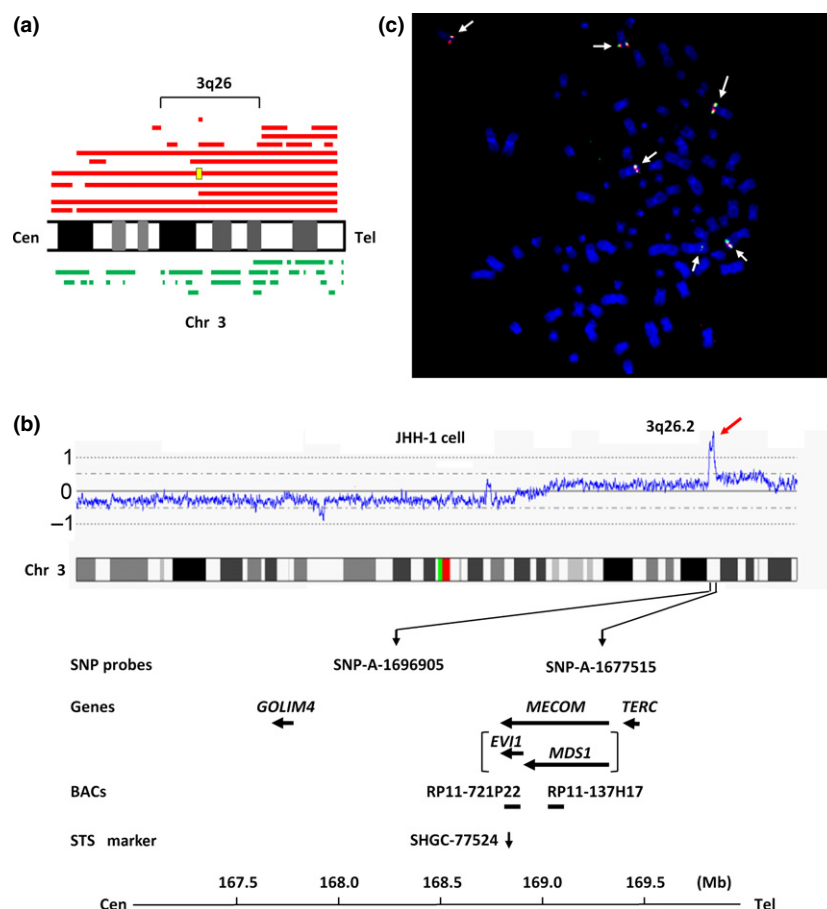
**DNA copy number and expression of *EV11* in HCC cell lines.** The DNA copy number of *EV11* was then determined in the

20 HCC cell lines by using quantitative PCR. The sequence-tagged site marker, SHGC-77524, which is specific for *EV11*, was used for this PCR (Fig. 1b). For this analysis, copy number changes were counted as gains if the copy number for a given tumor cell line exceeded the mean plus two standard deviations of that in normal lymphocytes. A copy number gain of *EV11* was observed in seven (35%) of the 20 cell lines (Fig. 2a). As expected, JHH-1 cells showed the highest copy number gain.

As *EV11*, *MDS1–EV11*, and *MDS1* can all be transcribed from the *MECOM* locus, we next determined which transcript might be the target that acts as a driving force for the 3q26 amplification. We therefore used different primer and probe combinations to discriminate between *EV11*, *MDS1–EV11*, and *MDS1* and quantified their transcript levels in 18 of the HCC cell lines using quantitative TaqMan PCR analysis. *EV11* and *MDS1–EV11*, but not *MDS1*, were overexpressed in JHH-1 cells relative to the other cell lines (Fig. 2b).

To confirm that enhanced *EV11* and *MDS1–EV11* transcription resulted in enhanced protein expression, we further analyzed *EV11* protein expression in a number of these cell lines. Immunoblot analysis using the anti-*EV11* antibody showed that *EV11* protein expression was upregulated in JHH-1 cells relative to the other cell lines (Fig. 2c). Three forms of *EV11* protein were detected: *MDS1–EV11*, *EV11*, and the truncated form of *EV11* (*EV11Δ*).<sup>(3)</sup> The *MDS1–EV11* protein is of higher molecular weight as it possesses 188 additional amino acids at its N-terminus, which is encoded by exon 1 and 2 of *MDS1* and exon 2 and the untranslated part of exon 3 of *EV11*, in addition to the entire *EV11* sequence.<sup>(16)</sup> Of these three forms, the *EV11* protein was the most prominent.

**Fig. 1.** Map of the amplicon at 3q26 in the JHH-1 hepatocellular carcinoma (HCC) cell line. (a) Recurrent copy number gains on the chromosomal region 3q26 in HCC cell lines assessed using a GeneChip Mapping array. Copy number gains are indicated by red horizontal lines above the chromosome ideogram. A high-level gain (amplification) is indicated by the yellow rectangle. Copy number losses are indicated by green lines under the chromosome ideogram. Each horizontal line represents an aberration detected in a single HCC cell line. (b) Copy number profile of chromosome (Chr) 3 in JHH-1 cells. The position of the Affymetrix single nucleotide polymorphism (SNP) probes, the genes present, the bacterial artificial chromosomes (BACs) used as probes for FISH experiments, and the sequence-tagged site (STS) marker used for real-time quantitative PCR are shown based on the University of California Santa Cruz genome database. (c) Representative images of FISH analysis of metaphase chromosomes from JHH-1 cells using the following bacterial artificial chromosome probes: paired RP11-721P22 (containing *EV11*; green) and RP11-137H17 (containing *MDS1*; red). The arrow indicates six signals each for red and green. Cen, centromere; Tel, telomere.



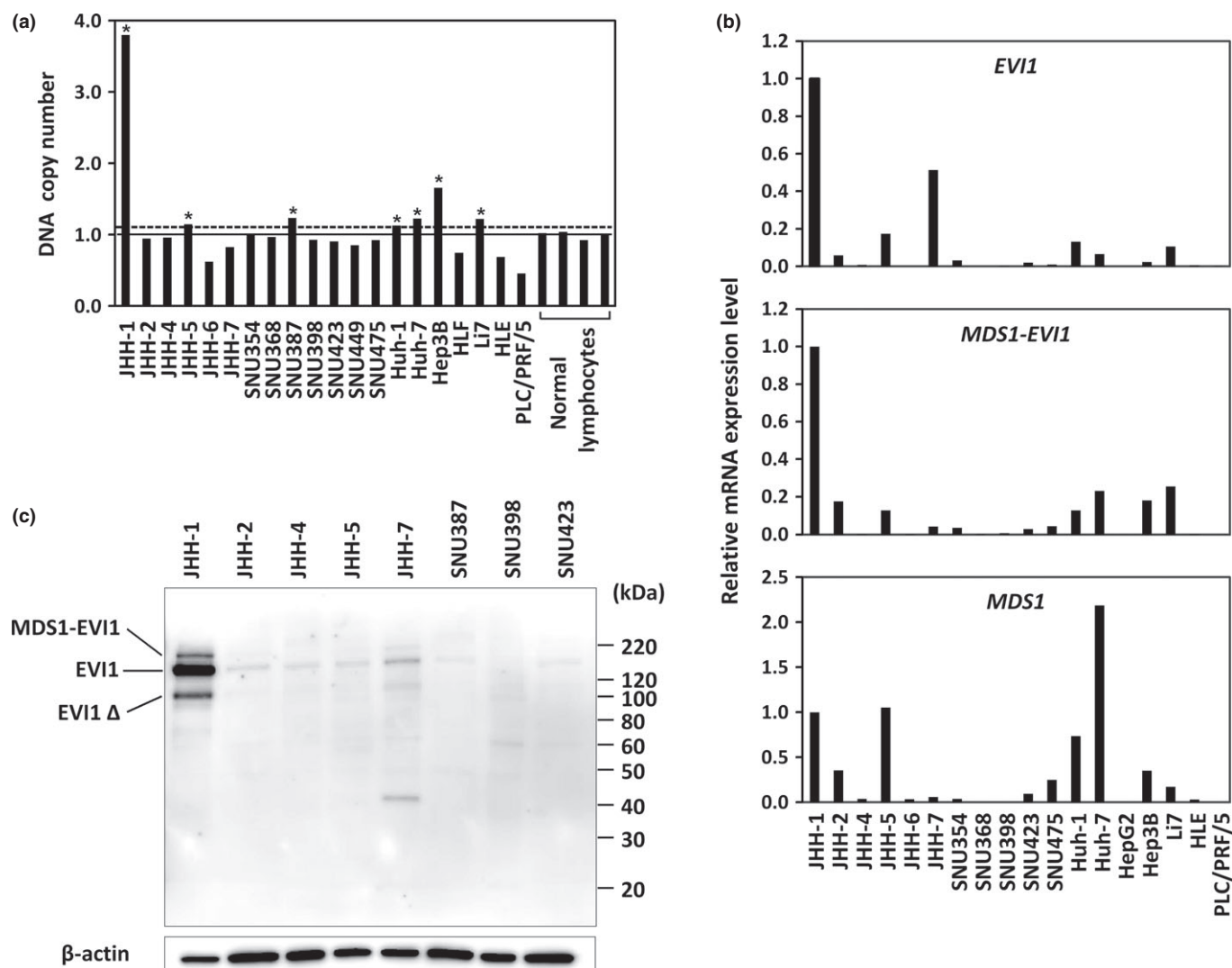


**Fig. 2.** DNA copy number of *EVI1*, mRNA levels of *EVI1*, *MDS1-EVI1*, and *MDS1*, and EVI1 protein expression in hepatocellular carcinoma (HCC) cell lines. (a) DNA copy number of *EVI1* in 20 HCC cell lines and four normal peripheral blood lymphocytes as measured by quantitative PCR. Values are normalized such that the average copy number in genomic DNA derived from four normal lymphocytes has a value of 1 (solid horizontal line). A value corresponding to the mean + two SD of the copy number of normal lymphocytes was used as the cut-off value for copy number gain (dotted line). Asterisks indicate cell lines showing copy number gain. (b) Relative levels of *EVI1*, *MDS1-EVI1*, and *MDS1* mRNAs in 18 HCC cell lines as determined by quantitative TaqMan PCR. (c) Immunoblot analyses of EVI1 protein in the indicated cell lines.  $\beta$ -actin was blotted as an internal control.

**DNA copy number and expression of *EVI1* in primary HCC tumors.** To determine whether the amplification of *EVI1* that was observed in JHH-1 cells was relevant to primary human carcinomas, the copy number of *EVI1* in primary HCC tumors was determined by quantitative PCR using a method similar to that used for the cell lines. A copy number gain of *EVI1* was observed in 24 (36%) of the 66 tumors (Fig. 3a).

Next, the mRNA levels of *EVI1*, *MDS1-EVI1*, and *MDS1* were measured in paired tumor and non-tumor liver tissues from 36 of the HCC patients using quantitative TaqMan PCR (Fig. 3b). *EVI1*, *MDS1-EVI1*, and *MDS1* mRNAs were detectable in 32, 25, and 5 of the 36 HCC tumors, respectively, and in 22, 19, and 1 of the 36 non-tumor liver tissues, respectively. Only *EVI1*, but not *MDS1-EVI1* or *MDS1*, was significantly overexpressed in 22 (61%) of the 36 HCC tumors when compared with their non-tumorous counterparts (Wilcoxon signed-rank test,  $P = 0.02$ ). These combined results suggest that *EVI1*

is a probable target for the 3q26 amplification in HCC. The copy numbers of *EVI1* in primary HCC tumors tended to correlate with *EVI1* mRNA levels, although the correlation was not statistically significant (Fig. S1).

To clarify the relationship between the elevated expression of *EVI1* in HCC tumors and various clinicopathological parameters, we correlated the *EVI1* expression level with available clinical data. For this purpose, tumors were divided into “high” and “low” expression groups with respect to the median mRNA level of *EVI1*. High *EVI1* expression was significantly associated with larger tumor size and higher level of DCP, which is also known as prothrombin induced by vitamin K absence-II (PIVKA-II) and is a tumor marker for HCC (Table 1). No significant correlations were apparent between the level of *EVI1* mRNA and other parameters, including age, sex, hepatitis B or hepatitis C virus infection,  $\alpha$ -fetoprotein level, and clinical stage. No relationship was observed between

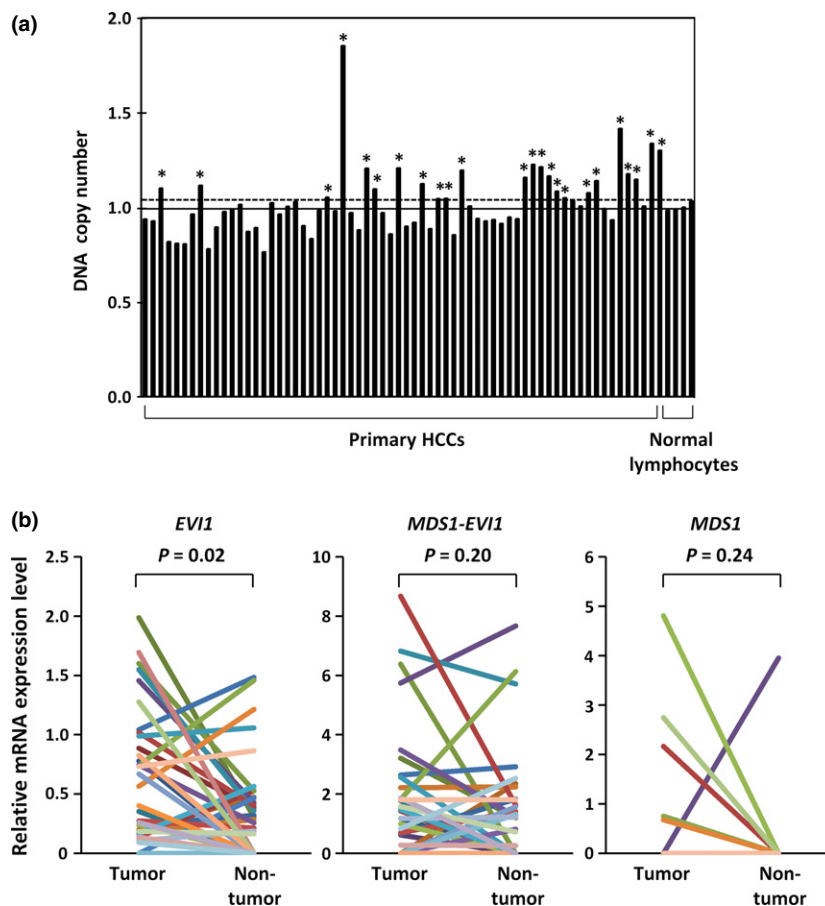


**Fig. 3.** DNA copy number of *EVI1* and mRNA levels of *EVI1*, *MDS1-EVI1*, and *MDS1* in primary hepatocellular carcinoma (HCC) tumors. (a) DNA copy number of *EVI1* in 66 primary HCC tumors and four normal peripheral blood lymphocytes was determined by quantitative PCR. \*Primary tumors showing copy number gain. (b) Relative levels of *EVI1*, *MDS1-EVI1*, and *MDS1* mRNA in paired tumor and non-tumor tissues from 36 patients with primary HCC.

the levels of *EVI1* mRNA and overall or disease-free survival (data not shown).

**Suppression of TGF- $\beta$ -mediated growth inhibition by *EVI1* in HCC cells.** The oncoprotein *EVI1* is known to suppress TGF- $\beta$  signaling by inhibiting Smad3 and to activate the PI3K/AKT and RAS/ERK signaling pathways. To determine whether *EVI1* affects any of these signaling pathways in HCC cells, *EVI1* protein expression in JHH-1 cells was knocked down using two different siRNAs (#1 and #2). *EVI1* siRNA (#1) was also used to knockdown the *EVI1* protein in a second cell line, JHH-7, that had the second highest level of *EVI1* expression (Fig. 2). Immunoblot analysis indicated successful knockdown of *EVI1* in all cases (Fig. 4a). Knockdown of *EVI1* using *EVI1* siRNA (#1) had little effect on the phosphorylated levels of AKT or ERK (data not shown), suggesting that *EVI1* does not regulate the PI3K/AKT or RAS/ERK signaling pathways. To assay if *EVI1* affects TGF- $\beta$  signaling in HCC cells, JHH-1 cells that were transfected with *EVI1* siRNA (#1) or control siRNA were treated with TGF- $\beta$  for 24 h, following which the mRNA expression of *PAI-1*, a classic TGF- $\beta$ -responsive gene, was analyzed using RT-PCR. The expression of *PAI-1* mRNA was induced by TGF- $\beta$  and was higher in JHH-1 cells treated with *EVI1* siRNA compared to those treated with control siRNA (Fig. 4b), suggesting that *EVI1* attenuates TGF- $\beta$ -mediated gene induction in JHH-1 cells.

Based on these data, we further examined the relationship between *EVI1* and components of the TGF- $\beta$  signaling pathway related to cell proliferation using the *EVI1* knockdown and control cells. The RT-PCR analysis of siRNA-control cells indicated that TGF- $\beta$  treatment induced p15<sup>INK4B</sup> mRNA and

decreased c-Myc mRNA expression in JHH-1 cells (Fig. 4b). Furthermore, TGF- $\beta$ -treated JHH-1 cells that were transfected with *EVI1* siRNA showed increased p15<sup>INK4B</sup> expression, and decreased c-Myc and cyclin D1 expression at both the mRNA and protein levels compared to TGF- $\beta$ -treated control siRNA cells (Fig. 4b,c). Consistent with these data, the level of phosphorylated Rb protein after TGF- $\beta$  treatment was lower in JHH-1 cells treated with *EVI1* siRNA compared to those treated with control siRNA (Fig. 4c). To rule out siRNA off-target effects and toxicity, we then confirmed these results using siRNA (#2) in JHH-1 cells and siRNA (#1) in JHH-7 cells (Fig. 4c). These data suggested that *EVI1* attenuates the induction of p15<sup>INK4B</sup> by TGF- $\beta$  and antagonizes TGF- $\beta$ -mediated repression of c-Myc and cyclin D1, resulting in decreased Rb phosphorylation. These effects of *EVI1* suggest that *EVI1* might inhibit TGF- $\beta$ -mediated inhibition of proliferation.

We therefore further examined the effect of *EVI1* knockdown on TGF- $\beta$  modulation of cell proliferation by analysis of BrdU incorporation. BrdU is known to be incorporated into the newly synthesized DNA of replicating cells during the S phase of the cell cycle. BrdU incorporation was significantly lower in TGF- $\beta$ -treated JHH-1 cells treated with *EVI1* siRNA (#1) compared to those treated with control siRNA (Fig. 4d). To confirm this finding, we next determined if overexpression of *EVI1* might enhance TGF- $\beta$  induced BrdU incorporation. We therefore transfected the *EVI1* expression vector into SNU398 cells (Fig. 4e), which showed little expression of *EVI1* (Fig. 2), and treated them with TGF- $\beta$ . Immunocytochemistry with triple staining for *EVI1*, BrdU, and DAPI showed that *EVI1* was expressed in the nuclei of a portion of

**Table 1. Relationship between clinicopathological features and levels of expression of *EVII* mRNA in 36 hepatocellular carcinomas**

Characteristic	<i>EVII</i> mRNA		P-value†
	Low (<median) (n = 18)	High (>median) (n = 18)	
Age, years	66 (44–79)	65 (35–77)	0.98
Sex			
Male	15	15	0.67
Female	3	3	
Tumor size, cm	4.5 (2.9–10.0)	5.7 (2.9–26.0)	0.03
Stage			
I, II, III	13	12	0.50
IV	5	6	
HBV infection			
Positive	5	4	0.50
Negative	13	14	
HCV infection			
Positive	9	9	0.63
Negative	9	9	
AFP, ng/mL	21.4 (0.9–114 859)	28.2 (2.4–94 560)	0.63
DCP, mAU/mL	100 (1–17 000)	1020 (18–111 000)	0.04

† $\chi^2$ -test or Mann–Whitney *U*-test. Values are medians (range) or numbers. Where no other unit is specified, values refer to numbers of patients. AFP,  $\alpha$ -fetoprotein; DCP, des- $\gamma$ -carboxy prothrombin; HBV, hepatitis B virus; HCV, hepatitis C virus.

SNU398 cells transfected with the *EVII* expression vector and that the *EVII*-expressing cells had a higher percentage of BrdU positive cells than cells without *EVII* expression (Fig. 4f,g). We next determined the effect of knockdown of *EVII* on the viability of TGF- $\beta$ -treated JHH-1 cells. Cell viability was assayed using the WST-8 assay after TGF- $\beta$  treatment of JHH-1 cells that were transfected with *EVII* siRNAs (#1 or #2) or control siRNA. Cell viability of all cells decreased in a time-dependent manner, because the cells were treated with TGF- $\beta$  in serum-free medium. However, the rate of decrease in cell viability was significantly faster in cells transfected with *EVII* siRNAs (#1 or #2) than in those transfected with control siRNA (Fig. 4h). These findings further suggested that *EVII* antagonizes TGF- $\beta$ -mediated growth inhibition. However, *EVII* knockdown did not inhibit the growth of JHH-1 cells under normal culture conditions in the absence of TGF- $\beta$  (data not shown).

Regarding other TGF- $\beta$  functions, *EVII* knockdown had little effect on TGF- $\beta$ -mediated induction of integrin  $\alpha$ 1, which is one of the earliest manifestations of EMT (data not shown). Moreover, TGF- $\beta$  treatment did not induce apoptosis in either the control or the *EVII* siRNA transfected JHH-1 cells as

assessed by cleavage of poly (ADP-ribose) polymerase, suggesting that *EVII* may not affect TGF- $\beta$ -mediated induction of apoptosis (data not shown).

## Discussion

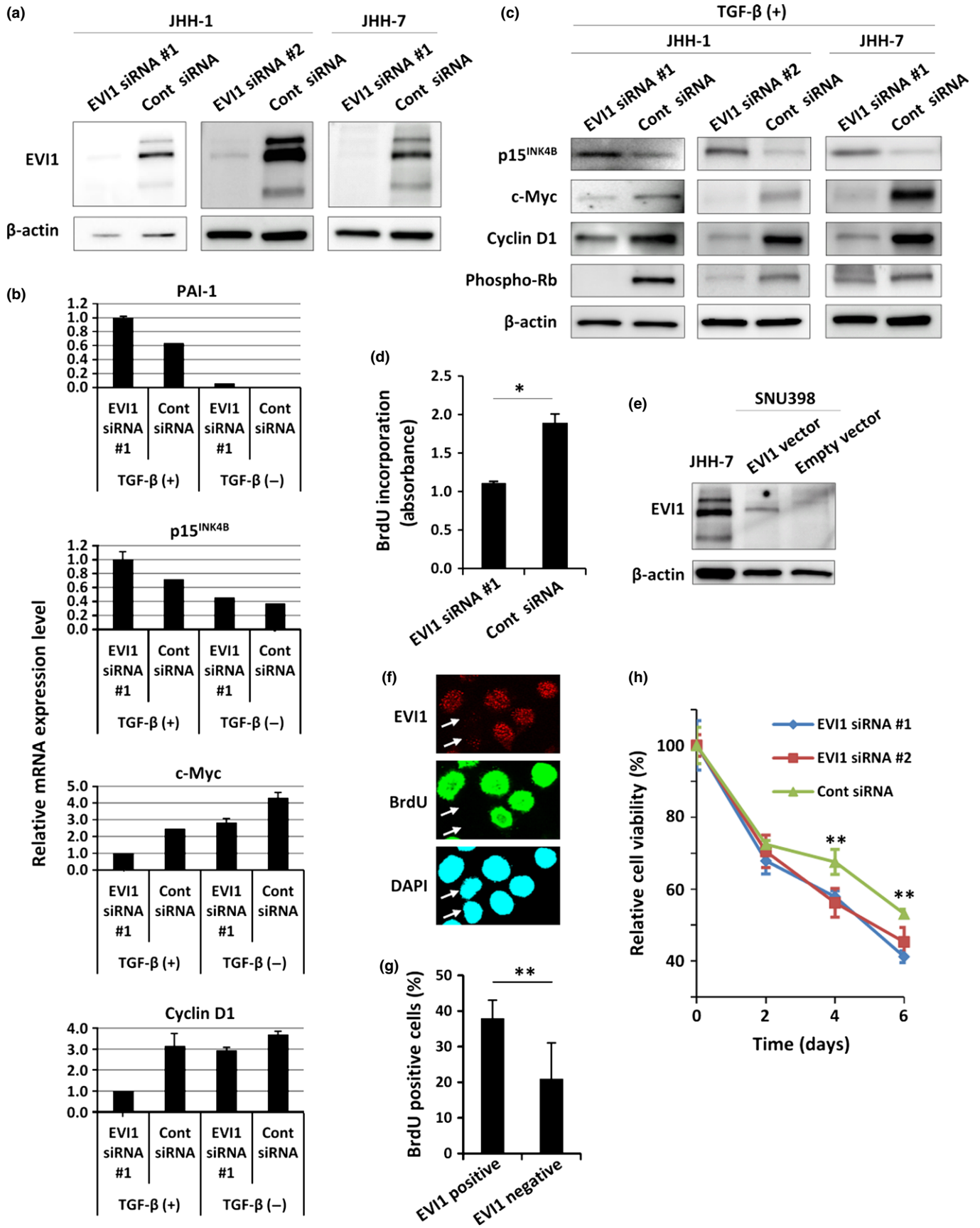
We identified a novel amplification at 3q26 in the HCC cell line JHH-1, and found that *EVII*, which lies within the 3q26 region, is amplified in these cells. A copy number gain of *EVII* was frequently observed in both a number of HCC cell lines and in primary HCCs. Subsequent experiments suggested that *EVII*, but not *MDS1–EVII* or *MDS1*, is the most likely target for the amplicon, as only the *EVII* transcript was overexpressed in JHH-1 cells and was significantly upregulated in primary HCC tumors when compared with non-tumorous counterparts. Moreover, we showed that *EVII* antagonizes TGF- $\beta$ -mediated growth inhibition in JHH-1 cells through attenuation of p15<sup>INK4B</sup> induction.

Increased DNA copy number involving 3q26 is frequently found in a number of epithelial cancers, suggesting that the 3q26 region harbors one or more target genes, the amplification of which renders them oncogenic. Potential target genes in the 3q26 amplicon have been identified in epithelial cancers, including *PIK3CA*,<sup>(17)</sup> *PKC $\alpha$* ,<sup>(18)</sup> and *EVII*<sup>(7)</sup> in ovarian cancer, *SOX2* in squamous cell lung cancer<sup>(19)</sup> and small-cell lung cancer,<sup>(20)</sup> and *FNDC3B*<sup>(21)</sup> in HCC. We previously identified *TERC*<sup>(22)</sup> and *SOX2*<sup>(23)</sup> as the targets for the 3q26 amplification in non-small-cell lung cancer and esophageal squamous cell carcinoma, respectively. Amplification of *EVII* has been found in primary ovarian cancers,<sup>(7,8)</sup> colon cancer cell lines,<sup>(9)</sup> and non-small-cell lung cancer cell lines.<sup>(22)</sup> However, to our knowledge, this is the first report to describe the amplification and overexpression of *EVII* in HCC.

Expression experiments in the present study showed that *EVII* and *MDS1–EVII* mRNAs were detectable in non-tumor liver tissues in approximately half of cases, whereas *MDS1* was rarely detected. It is known that *EVII* is highly expressed in adult hematopoietic stem cells.<sup>(24,25)</sup> Although *EVII* is also expressed in the hematopoietic stem/progenitor fraction in the fetal liver of mouse embryos,<sup>(26)</sup> the physiological function of *EVII* and *MDS1–EVII* in the adult liver is unknown. The function of *MDS1* also remains unknown.

Our results showed that high *EVII* expression was significantly associated with larger tumor size and higher level of DCP, a diagnostic and surveillance marker for HCC. It has been shown that DCP is a predictor of microvascular invasion, which is a major risk factor for tumor recurrence and mortality in HCC.<sup>(27)</sup> These observations supported the notion that upregulation of *EVII* might be involved in the progression of HCC. Unlike in myeloid leukemia, no relationship was observed between the levels of *EVII* mRNA and survival in

**Fig. 4.** Effect of *EVII* knockdown on transforming growth factor- $\beta$  (TGF- $\beta$ )-mediated growth inhibition in JHH-1 hepatocellular carcinoma cells. (a) Immunoblot analysis of *EVII* and  $\beta$ -actin, an internal control, in JHH-1 and JHH-7 cells transfected with *EVII* (#1) or *EVII* (#2) siRNA as indicated or with control siRNAs. (b) Relative mRNA expression levels of the indicated genes in JHH-1 cells that were transfected with *EVII* (#1) or control (Cont) siRNAs and were then treated with TGF- $\beta$ 1 (10 ng/mL) or vehicle for 24 h. (c) Immunoblot analysis of the indicated proteins in JHH-1 and JHH-7 cells that were transfected with *EVII* siRNA (#1 or #2 as indicated) or with control siRNA and were then treated with TGF- $\beta$ 1 for 24 h. (d) BrdU incorporation as determined by ELISA. JHH-1 cells transfected with *EVII* siRNA (#1) or control siRNA were treated with TGF- $\beta$ 1 for 24 h and were then labeled with BrdU for 6 h. \**P* < 0.01. (e) Immunoblot analysis of *EVII* in SNU398 cells transfected with the *EVII* expression vector or an empty vector. JHH-7 cells were used as a positive control. (f, g) SNU398 cells transfected with the *EVII* expression vector were treated with TGF- $\beta$ 1 for 12 h then labeled with BrdU for 12 h. (f) Immunofluorescence. The cells were triple-labeled with anti-*EVII* (red), anti-BrdU (green), and DAPI (blue; nuclei). In this image, *EVII*-positive cells were positive for BrdU, whereas *EVII*-negative cells were negative for BrdU (arrows). (g) Percentage of BrdU-positive cells in *EVII*-positive or -negative cells. More than 300 cells were counted for each group. \*\**P* < 0.05. (h) JHH-1 cells were transfected with *EVII* siRNA (#1 or #2) or control siRNA then treated with TGF- $\beta$ 1. Relative cell viability (%) is shown at the indicated times after TGF- $\beta$ 1 treatment. \*\**P* < 0.05.



our HCC patients. However, our sample size was too small to draw a definite conclusion. Further studies with more numerous primary samples are needed to determine the clinical importance of EVI1 in HCC.

Although the role of EVI1 in tumorigenesis has not been fully elucidated, it is suggested that EVI1 possesses diverse functions as an oncoprotein and affects cell proliferation and apoptosis in a cell-type specific manner. EVI1 can prevent apoptosis by negatively regulating the c-Jun N-terminal kinase pathway<sup>(28)</sup> or by activating the PIK3/AKT pathway.<sup>(9)</sup> Moreover, it can stimulate cell growth by activating the PIK3/AKT pathway<sup>(10)</sup> or the RAS/ERK pathway.<sup>(11)</sup> Our results showed that knockdown of *EVI1* resulted in increased induction of p15<sup>INK4B</sup> by TGF- $\beta$  and decreased expression of c-Myc, cyclin D1, and phosphorylated Rb. Consequently, knockdown of *EVI1* led to reduced BrdU incorporation and reduced cell viability, implying reduced cell proliferation. These findings suggested that EVI1 antagonizes TGF- $\beta$ -mediated growth inhibition in HCC cells and are consistent with a previous report that EVI1 suppresses TGF- $\beta$ -mediated growth inhibition.<sup>(12)</sup> Therefore, EVI1 may be involved in hepatocarcinogenesis, in part, through suppression of the TGF- $\beta$  signaling pathway. To determine if EVI1 expression might be associated with alterations in genes of the TGF- $\beta$  signaling pathway in the HCC cell lines that we used, we searched the Catalogue Of Somatic Mutations In Cancer database (<http://cancer.sanger.ac.uk/cancergenome/projects/cosmic/>) for mutations in such genes. This search indicated that the TGF- $\beta$  receptor 1 gene (*TGFBR1*) is mutated in JHH-1 cells, but not in JHH-7 or SNU398 cells. However, in our study, the fact that the expression of PAI-1 mRNA was strongly induced by TGF- $\beta$  in JHH-1 cells suggested that TGF- $\beta$  signaling was active in JHH-1 cells. No mutation in the TGF- $\beta$  receptor 2 gene (*TGFBR2*) or in the *Smad4* gene (*SMAD4*) is found in these three cell lines. Although other signaling pathways may be involved in the oncogenic role of EVI1 in HCC, we could not find evidence of the involvement of EVI1 with any pathway other than the TGF- $\beta$  pathway, at least, under the conditions of our experiments. Further studies are needed to determine the functional role of EVI1 in HCC and the exact mechanism by which EVI1 antagonizes TGF- $\beta$ -mediated growth inhibition in HCC cells.

Transforming growth factor- $\beta$  signaling has been shown to act as a tumor suppressor or a promoter in HCC in a context-dependent manner.<sup>(29,30)</sup> Transforming growth factor- $\beta$  inhibits the growth of hepatocytes, acting as a tumor suppressor. Because only a fraction of HCCs show inactivating mutations

in components of the TGF- $\beta$  signaling pathway, other mechanisms for perturbing TGF- $\beta$  signaling appear critical for the development of HCC. However, TGF- $\beta$  signaling promotes HCC progression and EMT by acting as an autocrine or paracrine growth factor and by inducing microenvironmental changes, including changes in the numbers of cancer-associated fibroblasts and T regulatory cells, and in the levels of inflammatory mediators. The switch of TGF- $\beta$  function from tumor suppression to promotion is not well understood. Most HCC arises on a background of cirrhosis, which is characterized by the accumulation of ECM proteins. The deposition of ECM is largely stimulated by TGF- $\beta$ . This tight interaction between the tumor and the surrounding cirrhotic liver is one of the most remarkable hallmarks of HCC.

In conclusion, we have identified *EVI1* as a novel target for the amplification event at 3q26 in HCC. Our results suggest that EVI1 antagonizes TGF- $\beta$ -mediated growth inhibition in HCC cells and could therefore represent a potential molecular target for the development of novel therapies to treat HCC.

### Acknowledgments

This study was supported by a Grant-in-Aid for Scientific Research (No. 20590408) (to K Yasui) from the Japan Society for the Program of Science.

### Disclosure Statement

The authors have no conflict of interest.

### Abbreviations

AKT	protein kinase B
AML	acute myeloid leukemia
BAC	bacterial artificial chromosome
CDK	cyclin-dependent kinase
DCP	des- $\gamma$ -carboxy prothrombin
EMT	epithelial–mesenchymal transition
EVI1	ecotropic viral integration site 1
HCC	hepatocellular carcinoma
MDS1	myelodysplastic syndrome 1
MECOM	MDS1 and EVI1 complex locus
phospho-Rb	phosphorylated Rb
PI3K	phosphatidylinositol 3-kinase
SNP	single nucleotide polymorphism
TGF- $\beta$	transforming growth factor- $\beta$

### References

- 1 Ferlay J, Shin HR, Bray F, Forman D, Mathers C, Parkin DM. Estimates of worldwide burden of cancer in 2008: GLOBOCAN 2008. *Int J Cancer* 2010; **127**: 2893–917.
- 2 Collins C, Rommens JM, Kowbel D *et al*. Positional cloning of ZNF217 and NABC1: genes amplified at 20q13.2 and overexpressed in breast carcinoma. *Proc Natl Acad Sci U S A* 1998; **95**: 8703–8.
- 3 Goyama S, Kurokawa M. Evi-1 as a critical regulator of leukemic cells. *Int J Hematol* 2010; **91**: 753–7.
- 4 Morishita K, Parker DS, Mucenski ML, Jenkins NA, Copeland NG, Ihle JN. Retroviral activation of a novel gene encoding a zinc finger protein in IL-3-dependent myeloid leukemia cell lines. *Cell* 1988; **54**: 831–40.
- 5 Barjesteh van Waalwijk van Doorn-Khosrovani S, Erpelinck C, van Putten WL *et al*. High EVI1 expression predicts poor survival in acute myeloid leukemia: a study of 319 de novo AML patients. *Blood* 2003; **101**: 837–45.
- 6 Brooks DJ, Woodward S, Thompson FH *et al*. Expression of the zinc finger gene EVI-1 in ovarian and other cancers. *Br J Cancer* 1996; **74**: 1518–25.

- 7 Nanjundan M, Nakayama Y, Cheng KW *et al*. Amplification of MDS1/EVI1 and EVI1, located in the 3q26.2 amplicon, is associated with favorable patient prognosis in ovarian cancer. *Cancer Res* 2007; **67**: 3074–84.
- 8 Sunde JS, Donniger H, Wu K *et al*. Expression profiling identifies altered expression of genes that contribute to the inhibition of transforming growth factor-beta signaling in ovarian cancer. *Cancer Res* 2006; **66**: 8404–12.
- 9 Liu Y, Chen L, Ko TC, Fields AP, Thompson EA. Evi1 is a survival factor which conveys resistance to both TGFbeta- and taxol-mediated cell death via PI3K/AKT. *Oncogene* 2006; **25**: 3565–75.
- 10 Yoshimi A, Goyama S, Watanabe-Okochi N *et al*. Evi1 represses PTEN expression and activates PI3K/AKT/mTOR via interactions with polycomb proteins. *Blood* 2011; **117**: 3617–28.
- 11 Tanaka M, Suzuki HI, Shibahara J *et al*. EVI1 oncogene promotes KRAS pathway through suppression of microRNA-96 in pancreatic carcinogenesis. *Oncogene* 2014; **33**: 2454–63.
- 12 Kurokawa M, Mitani K, Irie K *et al*. The oncoprotein Evi-1 represses TGF-beta signalling by inhibiting Smad3. *Nature* 1998; **394**: 92–6.
- 13 Weinberg Robert A. *The Biology of Cancer*, 2nd edn. New York: Garland Science, 2014.



- 14 Zen K, Yasui K, Nakajima T *et al.* ERK5 is a target for gene amplification at 17p11 and promotes cell growth in hepatocellular carcinoma by regulating mitotic entry. *Genes Chromosom Cancer* 2009; **48**: 109–20.
- 15 Endo M, Yasui K, Zen Y *et al.* Alterations of the SWI/SNF chromatin remodelling subunit-BRG1 and BRM in hepatocellular carcinoma. *Liver Int* 2013; **33**: 105–17.
- 16 Fears S, Mathieu C, Zeleznik-Le N, Huang S, Rowley JD, Nucifora G. Intergenic splicing of MDS1 and EVI1 occurs in normal tissues as well as in myeloid leukemia and produces a new member of the PR domain family. *Proc Natl Acad Sci U S A* 1996; **93**: 1642–7.
- 17 Shayesteh L, Lu Y, Kuo WL *et al.* PIK3CA is implicated as an oncogene in ovarian cancer. *Nat Genet* 1999; **21**: 99–102.
- 18 Eder AM, Sui X, Rosen DG *et al.* Atypical PKC $\alpha$  contributes to poor prognosis through loss of apical-basal polarity and cyclin E overexpression in ovarian cancer. *Proc Natl Acad Sci U S A* 2005; **102**: 12519–24.
- 19 Bass AJ, Watanabe H, Mermel CH *et al.* SOX2 is an amplified lineage-survival oncogene in lung and esophageal squamous cell carcinomas. *Nat Genet* 2009; **41**: 1238–42.
- 20 Rudin CM, Durinck S, Stawiski EW *et al.* Comprehensive genomic analysis identifies SOX2 as a frequently amplified gene in small-cell lung cancer. *Nat Genet* 2012; **44**: 1111–6.
- 21 Chen CF, Hsu EC, Lin KT *et al.* Overlapping high-resolution copy number alterations in cancer genomes identified putative cancer genes in hepatocellular carcinoma. *Hepatology* 2010; **52**: 1690–701.
- 22 Yokoi S, Yasui K, Iizasa T, Imoto I, Fujisawa T, Inazawa J. TERC identified as a probable target within the 3q26 amplicon that is detected frequently in non-small cell lung cancers. *Clin Cancer Res* 2003; **9**: 4705–13.
- 23 Gen Y, Yasui K, Zen Y *et al.* SOX2 identified as a target gene for the amplification at 3q26 that is frequently detected in esophageal squamous cell carcinoma. *Cancer Genet Cytogenet* 2010; **202**: 82–93.
- 24 Chen W, Kumar AR, Hudson WA *et al.* Malignant transformation initiated by Mll-AF9: gene dosage and critical target cells. *Cancer Cell* 2008; **13**: 432–40.
- 25 Goyama S, Yamamoto G, Shimabe M *et al.* Evi-1 is a critical regulator for hematopoietic stem cells and transformed leukemic cells. *Cell Stem Cell* 2008; **3**: 207–20.
- 26 Kataoka K, Sato T, Yoshimi A *et al.* Evi1 is essential for hematopoietic stem cell self-renewal, and its expression marks hematopoietic cells with long-term multilineage repopulating activity. *J Exp Med* 2011; **208**: 2403–16.
- 27 Shirabe K, Itoh S, Yoshizumi T *et al.* The predictors of microvascular invasion in candidates for liver transplantation with hepatocellular carcinoma-with special reference to the serum levels of des-gamma-carboxy prothrombin. *J Surg Oncol* 2007; **95**: 235–40.
- 28 Kurokawa M, Mitani K, Yamagata T *et al.* The evi-1 oncoprotein inhibits c-Jun N-terminal kinase and prevents stress-induced cell death. *EMBO J* 2000; **19**: 2958–68.
- 29 Matsuzaki K, Seki T, Okazaki K. TGF- $\beta$  signal shifting between tumor suppression and fibro-carcinogenesis in human chronic liver diseases. *J Gastroenterol* 2014; **49**: 971–81.
- 30 Giannelli G1, Villa E, Lahn M. Transforming growth factor- $\beta$  as a therapeutic target in hepatocellular carcinoma. *Cancer Res* 2014; **74**: 1890–4.

## Supporting Information

Additional supporting information may be found in the online version of this article:

**Fig. S1.** Correlation between copy numbers and relative mRNA expression levels of EVI1.

**Table S1.** Primers and probes used for PCR.